JOBS
مجلة العلوم الأساسية
Journal of Basic Science
Print -ISSN 2306-5249
Online-ISSN 2791-3279
العدد الثامن والعشرون
٢٠٢٥م /١٤٤٦هـ
العدد الثامن والعشرون
(713) (699)

# تأثير الدوران في النقل التمعجي للمواد النانوية الهجينة في قناة مائلة مدببة

هناء عبدالحسين
جامعة واسط /كلية التربية الأساسية
hshatty@uowasit.edu.iq

**المستخلص :**

تبحث هذه الدراسة في كيفية تأثير دوران التدفق التمعجي للإشعاع الحراري غير الخطي على المواد النانوية الهجينة التي تمر عبر وسط مسامي داخل قناة. ويتم ذلك بتطبيق مجال مغناطيسي في قناة مدببة مائلة، مع مراعاة تأثير المجال المغناطيسي الهيدروديناميكي (MHD). تُفحص المعادلة الحاكمة من خلال تطبيق افتراضات الطول الموجي الطويل وتقريبات رينولدز المنخفضة. أجرينا دراسة تحليلية باستعمال برنامج ماثيماتيكا (١١.٣). توضح الرسوم البيانية ظاهرة احتجاز الفقاعات الدائرية فيما يتعلق بخطوط التدفق، والسرعة، ودرجة الحرارة، وتدرج الضغط. كما استُعملت جسيمات نانوية من المواد النانوية الهجينة لتأثيراتها. يعمل الماء كسائل أساسي، بينما تتكون الجسيمات النانوية من البوليسترين وأكسيد الجرافين. تُظهر النتائج أن السرعة تزداد مع زيادة دوران السائل $\Omega$ ، بينما يتناقص تدرج الضغط. ترتفع درجة الحرارة بزيادة معامل امتصاص الحرارة $\beta$ ، بينما تنخفض بزيادة معامل الانزلاق الحراري $\gamma$ .

**الكلمات المفتاحية:** النقل التمعجي، مادة نانوية هجينة، الدوران، قناة مدببة.

# Influences of Rotation in Peristaltic Transport of Hybrid Nanomaterial in an Inclined Tapered Channel

**Hanaa Abdulhussein**
Wasit University/College of Basic Education
hshatty@uowasit.edu.iq

**Abstract:**

This study investigates how the rotation of peristaltic flow of nonlinear thermal radiation affects hybrid nanomaterials that are passed via a porous

JOBS مجلة العلوم الأساسية
Journal of Basic Science
Print -ISSN 2306-5249
Online-ISSN 2791-3279
العدد الثامن والعشرون
٢٠٢٥م /١٤٤٦هـ

medium within a conduit. This process takes place while applying a magnetic field in an inclined tapered canal and thinking about the impact of the magnetohydrodynamic (MHD) field. The governing equation is examined through the application of long-wavelength assumptions and low Reynolds approximations. We carried out an analytical investigation using the Mathematica (11.3) software. The graphs illustrate the phenomenon of trapping circular bubbles in relation to flow lines, velocity, temperature, and pressure gradient. Hybrid nanomaterial nanoparticles are also employed for their impacts. Water serves as the base liquid, while the nanoparticles consist of polystyrene and graphene oxide. The findings demonstrate that velocity rises with an increase in fluid rotation $\Omega$, whereas the pressure gradient diminishes. The temperature rises with an increase in the heat absorption parameter $\beta$ , whereas it declines with an increase in the thermal slip parameter $\gamma$.

**1. Introduction**

Peristaltic pumping is a form of fluid movement that occurs when a progressive wave gets interwoven inside an area. (Latham, 1966) pioneered peristaltic transfer in his initial endeavour. The laboratory model for the peristalsis process was initially introduced by (Fung & Yih , 1968). A substantial body of literature on peristalsis currently exists. See references for a variety of fluid models and flow configurations (Shapiro et al., 1969), (Abdulhussein & Abdulhadi, 2023) and (Ibraheem & Hummady, 2024). Water flow is a Newtonian fluid and serves as an exemplary illustration of peristaltic flow. Due to the peristaltic motion mechanism and its widespread application in medical engineering and the healthcare sector, Recent researchers have conducted thorough examinations.

Researchers designate the resulting nanofluids as hybrid nanomaterial fluids after examining the suspension of various combinations of nanoparticles with base fluids. Characterized as distinct chemical conjugates comprising organic and/or inorganic substances. The findings indicate an unusual increase in thermal conductivity at the fluid's base, even with a modest concentration of nanoparticles. The nanoparticles and slip characteristics in the peristaltic motion of magneto-hybrid nanofluids. by

JOBS
مجلة العلوم الأساسية
Journal of Basic Science
Print -ISSN 2306-5249
Online-ISSN 2791-3279
العدد الثامن والعشرون
٢٠٢٥م /١٤٤٦هـ

(Iftikhar et al., 2019) and (Sheriff et al., 2021) initially addressed the influence of connectivity in hybrid nanofluid flow in thermally conductive fluids with a low concentration of nanoparticles, as (Zahan et al., 2019) demonstrated in their examination of heat energy in hybrid nanofluids. The preliminary discourse on the mechanism of peristaltic transport naturally extends to the expansion and contraction of a symmetric channel. (Abbasi et al., 2020) and (Imran et al., 2020) examined the peristaltic flow of fluid through the characteristics of nanomaterials. Researchers have demonstrated the high effectiveness of the peristalsis mechanism in fluid transfer. (Nazeer et al., 2023) and (Noreen et al., 2017) tackled an issue related to Electroosmotic processes influence the transmission of heat and generation of entropy in blood flow, which includes gold nanoparticles, within an asymmetrical channel. The magnetohydrodynamic and thermal aspects of peristaltic flow have piqued the interest of numerous researchers (Sheriff et al., 2021), (Salih & Abdulhadi, 2024) and (Salman, 2023) since their examination.

The phenomenon of rotation has various applications in cosmological and geophysical processes and enhances our understanding of galaxy formation and ocean circulation. Overview of research evaluating the effects of the rotation ensues. Researchers have lately investigated the influence of a magnetic fields and rotational forces on fluid dynamics within non-symmetric canals, as noted by (Abd-Alla & Abo-Dahab, 2015) and (Alshareef, 2020).

This study examines the effects of rotation in peristaltic movement of hybrid nanomaterials fluid within a inclined tapered canal through a porous medium. The axial velocity, temperature, pressure gradient and trapping phenomenon results for various critical parameters in our inquiry have been analyzed using the system of nonlinear equations. By applying long-wavelength assumptions and low Reynolds approximations, this paper investigates the governing equation.

## 2. Mathematical Structure of the Model

JOBS
مجلة العلوم الأساسية
Journal of Basic Science
Print -ISSN 2306-5249
Online-ISSN 2791-3279
العدد الثامن والعشرون
٢٠٢٥م /١٤٤٦هـ

It is important to note that the influences of rotation and magnetic fields can be effectively analyzed via a porous medium with an inclined tapered canal composed of hybrid nanomaterial. See Fig.1.

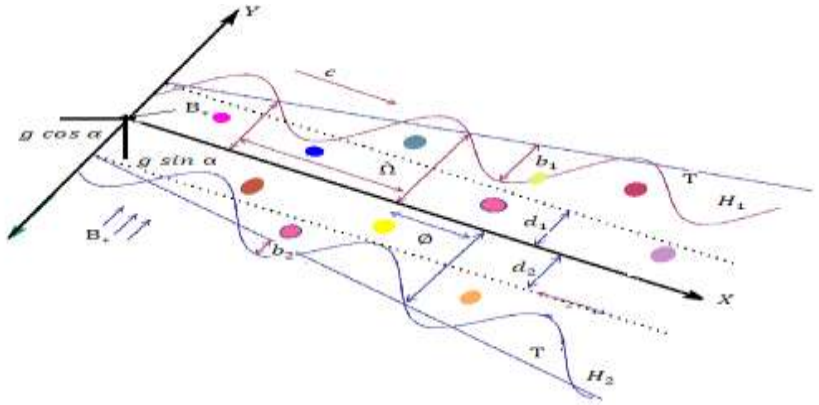


**Figure 1.** Geometry of the problem

$$H_1(X,t) = d_1 + \bar{m}X + b_1\, Sin\left[\frac{2\pi}{\lambda}(X - ct)\right] \quad (1)$$

$$H_2(X,t) = -d_2 - \bar{m}X - b_2\, Sin\left[\frac{2\pi}{\lambda}(X - ct) + \phi\right] \quad (2)$$

where $t, b_1, b_2, \bar{m}, c, \lambda$ are the time, amplitudes of waves, non-uniform parameter, wave speed and wavelength, $\emptyset$ $(0 \le \emptyset \le \pi)$ represents the phase difference between the walls of the channel, utilizing the rectangular Cartesian coordinates $X$ and $Y$. aligns the channel's axis $X$, while $Y$, which is perpendicular to $X$, aligns the transverse axis. We denote the constant heights of the upper and lower walls from the central line as $d_1$ and $d_2$, respectively and we angle the width of the channel wells with respect to the central axis $X$. Notably, $\phi = 0$ denotes asymmetry with out-of-phase waves, whereas $\phi = \pi$ pertains to waves that are in phase. Moreover, $d_1$ , $d_2$, $b_1$, $b_2$and $\phi$ . the following relationship is:

$$b_1^2 + b_2^2 + 2b_1 b_2 cos\phi \le (d_1 + d_2)^2 \quad (3)$$

The equations that govern.

$$\frac{\partial \mathrm{U}}{\partial \mathrm{X}} + \frac{\partial \mathrm{V}}{\partial \mathrm{Y}} = 0 \quad (4)$$

$$\rho_{ef}\left(\frac{\partial \mathrm{U}}{\partial t} + \mathrm{U}\frac{\partial \mathrm{U}}{\partial X} + \mathrm{V}\frac{\partial \mathrm{U}}{\partial Y}\right) - \rho_{ef}\dot{\Omega}\left(\dot{\Omega}U + 2\frac{\partial V}{\partial t}\right) = -\frac{\partial P}{\partial X} + \frac{\partial}{\partial X}\left(2\mu_{ef}\frac{\partial U}{\partial X}\right) + \frac{\partial}{\partial Y}\left(\mu_{ef}\left(\frac{\partial U}{\partial X} + \frac{\partial U}{\partial Y}\right)\right) - \sigma_{ef}B_*^2 U - \frac{\mu_{ef}}{k_\circ}\mathrm{U} + \rho_{ef}g\, sin\,\alpha$$

(5)

JOBS مجلة العلوم الأساسية Journal of Basic Science
Print -ISSN 2306-5249
Online-ISSN 2791-3279
العدد الثامن والعشرون
٢٠٢٥م /١٤٤٦هـ

$$\rho_{ef}\left(\frac{\partial V}{\partial t}+U\frac{\partial V}{\partial X}+V\frac{\partial V}{\partial Y}\right)-\rho_{ef}\dot{\Omega}\left(\dot{\Omega}V-2\frac{\partial U}{\partial t}\right)=-\frac{\partial P}{\partial Y}+\frac{\partial}{\partial X}\left(2\mu_{ef}\frac{\partial V}{\partial X}\right)+\frac{\partial}{\partial Y}\left(\mu_{ef}\left(\frac{\partial V}{\partial X}+\frac{\partial V}{\partial Y}\right)\right)-\frac{\mu_{ef}}{k_{\circ}}\mathrm{V}-\rho_{ef}\,g\,\cos\alpha \quad (6)$$

$$\left(\rho C_p\right)_{ef}\left(\frac{\partial \mathrm{T}}{\partial t}+\mathrm{U}\frac{\partial \mathrm{T}}{\partial X}+\mathrm{V}\frac{\partial \mathrm{T}}{\partial Y}\right)=k_{ef}\left(\frac{\partial^2 \mathrm{T}}{\partial X^2}+\frac{\partial^2 \mathrm{T}}{\partial Y^2}\right)+Q_{\circ} \quad (7)$$

where $\vec{V}$=$(U, \mathrm{V}, 0)$ represent velocity vector, $\dot{\Omega}=\Omega\dot{k}$ , $\dot{k}$ is the unit vector parallel to $Z$ axis , $\Omega$ is rotation, $P$ represents fluid pressure, $\rho_{ef}$ effective density, $\mu_{ef}$ effective dynamic viscosity, $\left(C_p\right)_{ef}$ is heat capacitance, T temperature, $k_{\circ}$ the permeability coefficient, $g$ gravitational acceleration, $\sigma_{ef}$ effective electrical conductivity, $k_{ef}$ effective thermal conductivity. The produced electric field is disregarded entirely due to the assumption of a low magnetic Reynolds number.

The steady flow occurs when we shift with constant (c)wave propagation speed from the fixed frame of reference $(X, Y)$ to the wave frame of reference$(\dot{x}, \dot{y})$ . Then using the wave frame transformations

$$\dot{v}=\mathrm{V}\ ,\ \dot{y}=Y\ ,\ \dot{\mathrm{T}}=\mathrm{T}\ ,\ \dot{x}=X-ct,\ \dot{u}=\mathrm{U}-c\ ,\ \dot{p}=P \quad (8)$$

By introducing the dimensionless parameter:

$$x=\frac{\dot{x}}{\lambda},\ y=\frac{\dot{y}}{d_1},\ \eta_1(x)=\frac{H_1}{d_1},\ \eta_2(x)=\frac{H_2}{d_1},\ \vartheta=\frac{\dot{\mathrm{T}}-\dot{\mathrm{T}}_0}{\dot{\mathrm{T}}_0},\ u=\frac{\dot{u}}{c},\ v=\frac{\lambda\dot{v}}{cd_1},\ \mathrm{t}=\frac{c\dot{t}}{\lambda},\ R_e=\frac{\rho_{ef}d_1c}{\mu_f},\ \delta=\frac{d_1}{\lambda},\ H=\mathrm{B}_{*}d_1\sqrt{\frac{\sigma_f}{\mu_f}},\ D_a=\frac{k_o}{d_1^2},\ F_r=\frac{c^2}{gd_1},\ p=\frac{d_1^2\,\dot{p}(\dot{x})}{\lambda\mu_f c},\ d=\frac{d_2}{d_1},\ m=\frac{\bar{m}}{d_1},\ a_1=\frac{b_1}{d_1},\ a_2=\frac{b_2}{d_1},\ \beta=\frac{Q_{\circ}d_1^2}{k_f\dot{T}_0},\ M=\frac{\mu_{ef}}{\mu_f},\ W=\frac{\sigma_{ef}}{\sigma_f},\ K=\frac{k_{ef}}{k_f} \quad (9)$$

where $M, W, K$ are represent mathematically from effective dynamic viscosity of hybrid nanomaterial, effective thermal diffusivity of hybrid nanomaterial, effective thermal conductivity of hybrid nanomaterial. Further,

JOBS مجلة العلوم الأساسية Journal of Basic Science
Print -ISSN 2306-5249
Online-ISSN 2791-3279
العدد الثامن والعشرون
٢٠٢٥م /١٤٤٦هـ

$H, D_a, R_e, \delta, F_r, \beta, \vartheta$ are represent Hartmann number, Darcy number, Reynolds number, Wave number , Froude number, heat absorption parameter, temperature, respectively.

experimental formulation for the physical characteristics of hybrid nanomaterial are show in Table (1), which are given by (Sheriff et al., 2021).

| physical characteristics | $(C_p)_f\ (J/kgK)$ | $\rho_f\ (kg/m^3)$ | $k_f\ (w/mK)$ | $\sigma_f\ (I/K)$ |
|---|---|---|---|---|
| Pure water | 1210 | 1053 | 0.16 | 0.05 x $10^{-5}$ |
| Polystyrene | 2430 | 1115 | 0.253 | 6.7 x $10^{-14}$ |
| Graphene oxide | 2090 | 783 | 0.145 | 1.03 x $10^{2}$ |

**Table 1.** Thermo-physical features of nanoparticles with base fluid.

The dimensionless configuration of the peristaltic canal walls is represented by $\eta_1(x)$ and $\eta_2(x)$as per equations (1) and(2).

$$\eta_1(x) = 1 + mx + a_1\ \mathrm{Sin}(2\pi x) \quad (10)$$

$$\eta_2(x) = -d - mx - a_2\ \mathrm{Sin}(2\pi x + \emptyset) \quad (11)$$

And relation $a^2 + b^2 + 2abcos\phi_\circ \leq (1+d)^2$ (12)

Where $\psi$ is the stream function for the components of velocity $u$ and $v$, defined as without dimension quantities: $u = \frac{\partial \psi}{\partial y}$ and $v = -\frac{\partial \psi}{\partial x}$.

We get the follow equations:

$$\frac{\partial p}{\partial x} = \frac{\mu_{ef}}{\mu_f}\frac{\partial^3 \psi}{\partial y^3} + \frac{\rho_{ef}\Omega^2 d_1^2}{\mu_f}\left(\frac{\partial \psi}{\partial y} + 1\right) - H^2\ \frac{\sigma_{ef}}{\sigma_f}\left[\left(\frac{\partial \psi}{\partial y} + 1\right)\right] - \frac{\mu_{ef}}{\mu_f}\frac{1}{D_a}\left(\frac{\partial \psi}{\partial y} + 1\right) + \frac{R_e}{F_r}\mathrm{Sin}\,\alpha \quad (13)$$

$$\frac{\partial p}{\partial y} = 0 \quad (14)$$

Upon differentiation (13), we obtain an equation devoid of the pressure gradient factor as:

JOBS مجلة العلوم الأساسية Journal of Basic Science
Print -ISSN 2306-5249
Online-ISSN 2791-3279
العدد الثامن والعشرون
٢٠٢٥م /١٤٤٦هـ

$$M\frac{\partial^4\psi}{\partial y^4}+\left[\frac{\rho_{ef}\,\Omega^2 d_1^2}{\mu_f}-W.H^2-\frac{M}{D_a}\right]\frac{\partial^2\psi}{\partial y^2}=0 \qquad (15)$$

$$\frac{\partial^2\vartheta}{\partial y^2}\,K+\beta=0 \qquad (16)$$

In the wave frame, the boundary conditions that do not include dimensions are (Salih & Abdulhadi, 2024):

$$\frac{\partial^2\psi}{\partial y^2}=0\,,\ \psi=0\,,\ \frac{\partial\vartheta}{\partial y}=0 \quad \text{at } y=\eta_1$$
$$\frac{\partial\psi}{\partial y}=-1,\ \psi=F\,,\ \vartheta+\gamma\frac{\partial\vartheta}{\partial y}=0 \quad \text{at } y=\eta_2 \qquad (17)$$

The resolution of equations (15) and (16) satisfies the corresponding boundary conditions (17).

$$\psi = r3+yr4+\frac{e^{-\frac{y\sqrt{(M+H^2D_aW)\mu_f-D_a\Omega^2d_1^2\rho_{ef}}}{\sqrt{M}\sqrt{S}\sqrt{\mu_f}}}\,MD_a(r1+e^{\frac{2y\sqrt{(M+H^2D_aW)\mu_f-D_a\Omega^2d_1^2\rho_{ef}}}{\sqrt{M}\sqrt{S}\sqrt{\mu_f}}}\,r2)\mu_f}{(M+H^2D_aW)\mu_f-D_a\Omega^2d_1^2\rho_{ef}} \qquad (18)$$

$$\vartheta=-\frac{y^2\beta}{2K}+\mathrm{C1}+y\mathrm{C2} \qquad (19)$$

Such that (r1, r2, r3, r4, C1,C2) the values of coefficient are large expressions.

Volumetric flow rate is assessed by means of

$$F=\int_{\eta_2}^{\eta_1}\psi\,\mathrm{dy}=\int_{\eta_2}^{\eta_1}\frac{\partial u}{\partial y}dy \qquad (20)$$

## 3 . Graphical Results and Discussion

In this area, we examined the impact of several parameters on the trapping phenomena, velocity distribution, pressure gradient, and temperature profile with a particular focus on the rotation parameter $\Omega$, Darcy number $D_a$, Hartmann number$H$, non-uniform parameter $m$ , effective density $\rho_{ef}$, effective thermal conductivity of hybrid nanomaterial $K$, thermal slip parameter $\gamma$ and heat absorption parameter $\beta$.

JOBS
مجلة العلوم الأساسية
Journal of Basic Science
Print -ISSN 2306-5249
Online-ISSN 2791-3279
العدد الثامن والعشرون
٢٠٢٥م/١٤٤٦هـ

3.1. Trapping Phenomena

To shed light on the phenomenon of entrapment, a circulating bolus of fluid is formed at the wave's velocity within a confined streamline zone. The phenomenon of trapping reduces the fluid's velocity to zero at particular locations within the wave framework. By accounting for the differences in the values of the stream function at the two specified locations, we are able to calculate the volumetric flow rate that is present over a line that connects multiple locations. This underscores the great significance of investigating simplified structures. The Lorentz force, acting against the fluid flow, decreases the size of the trapped mass in Figure (2), while as the Hartmann number $H$ increases. This paper concludes this finding. See how the Darcy number $D_a$, rotation $\Omega$, and non-uniform parameter $m$ behave in the opposite direction as they are increased in the figures (3-5). We observe an increase in the size of the trapped mass.

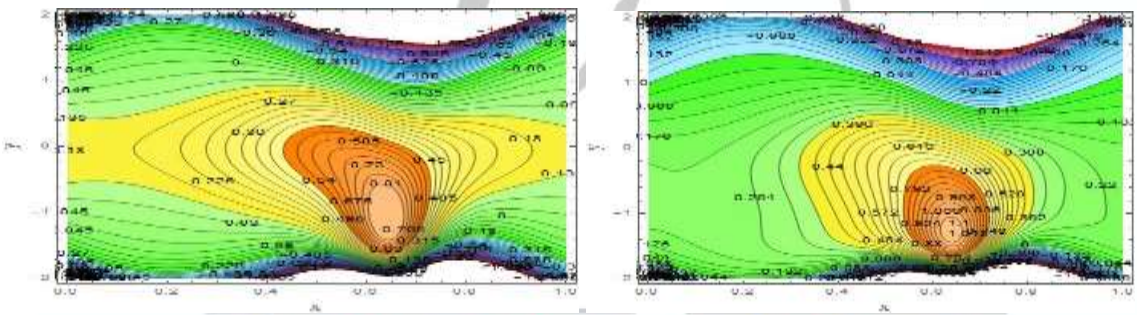

(a) (b)

**Figure 2.** Effect $H$ on the stream lines "$\psi$" for (a) "$H$" = 1 (b) "$H$" = 3

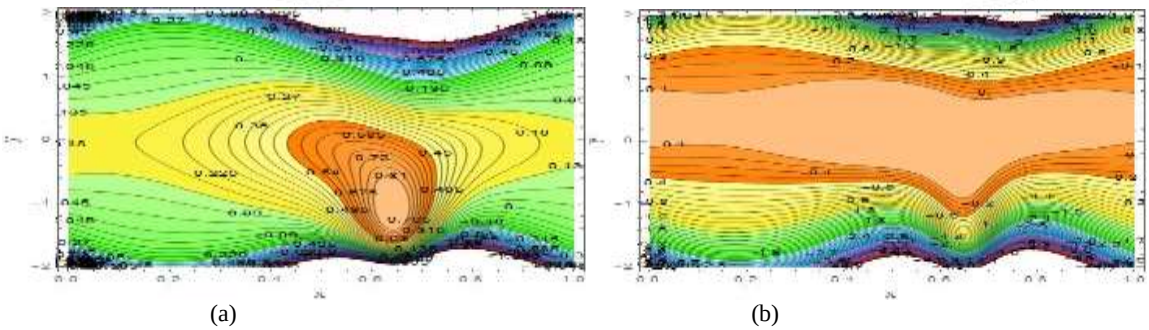

(a) (b)

**Figure 3.** Effect $D_a$ on the stream lines "$\psi$" for (a) "$D_a$" =1 (b) "$D_a$" =3

JOBS
مجلة العلوم الأساسية
Journal of Basic Science
Print -ISSN 2306-5249
Online-ISSN 2791-3279
العدد الثامن والعشرون
٢٠٢٥م/ ١٤٤٦هـ

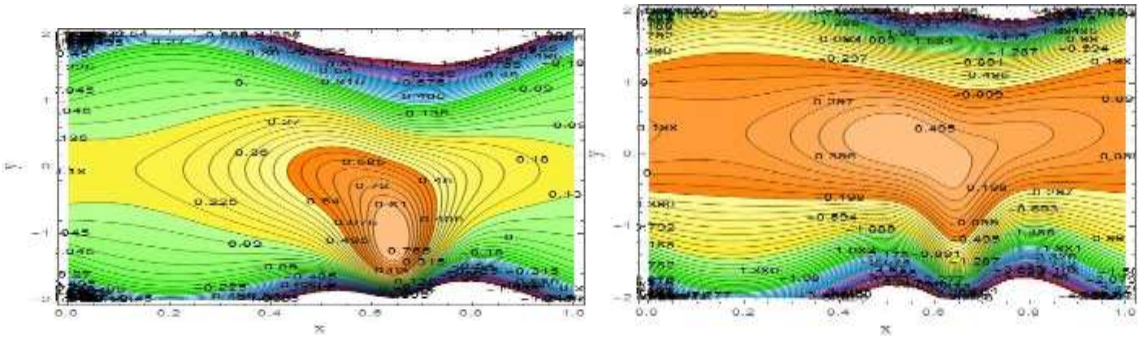

(a) (b)

**Figure 4.** Effect $\Omega$ on the stream lines "$\psi$" for (a) "$\Omega$" =1 (b) "$\Omega$" =7

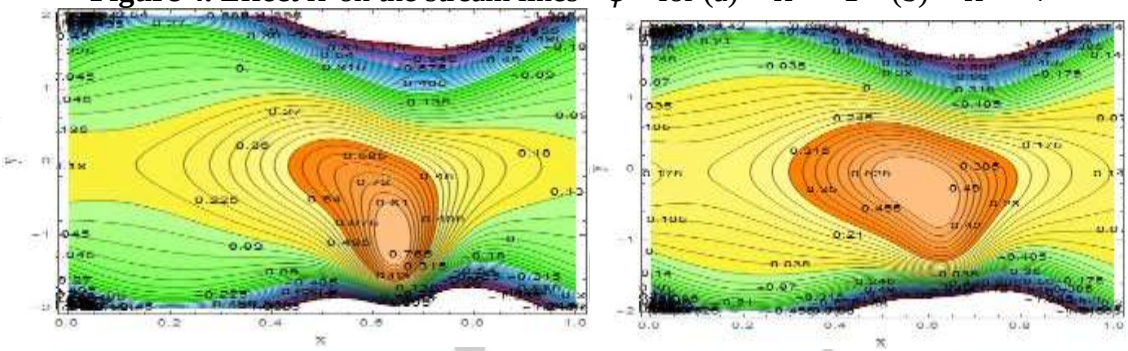

(a) (b)

**Figure 5.** Effect $m$ on the stream lines "$\psi$" for (a) "$m$" =0.1 (b)"$m$" =0.4

## 3.2. Velocity Profile

The influence of different values on axial velocity $u$ is illustrated in Figures 8 to show the effect of changing the values of Figure 6 (a- c). As this figure shows, Darcy number$D_a$ , rotation parameter $\Omega$ , and effective density $\rho_{ef}$go up, the axial velocity the axial velocity increases in the center of the channel. Figure 6 (d), shows that as the Hartmann number $H$ goes up, the axial velocity decreases in the middle of the channel. Figure 6(e) shows that when non-uniform parameter $m$ increases, the velocity decreases on the left side and increases on the right side.

JOBS
مجلة العلوم الأساسية
Journal of Basic Science
Print -ISSN 2306-5249
Online-ISSN 2791-3279
العدد الثامن والعشرون
٢٠٢٥م /١٤٤٦هـ

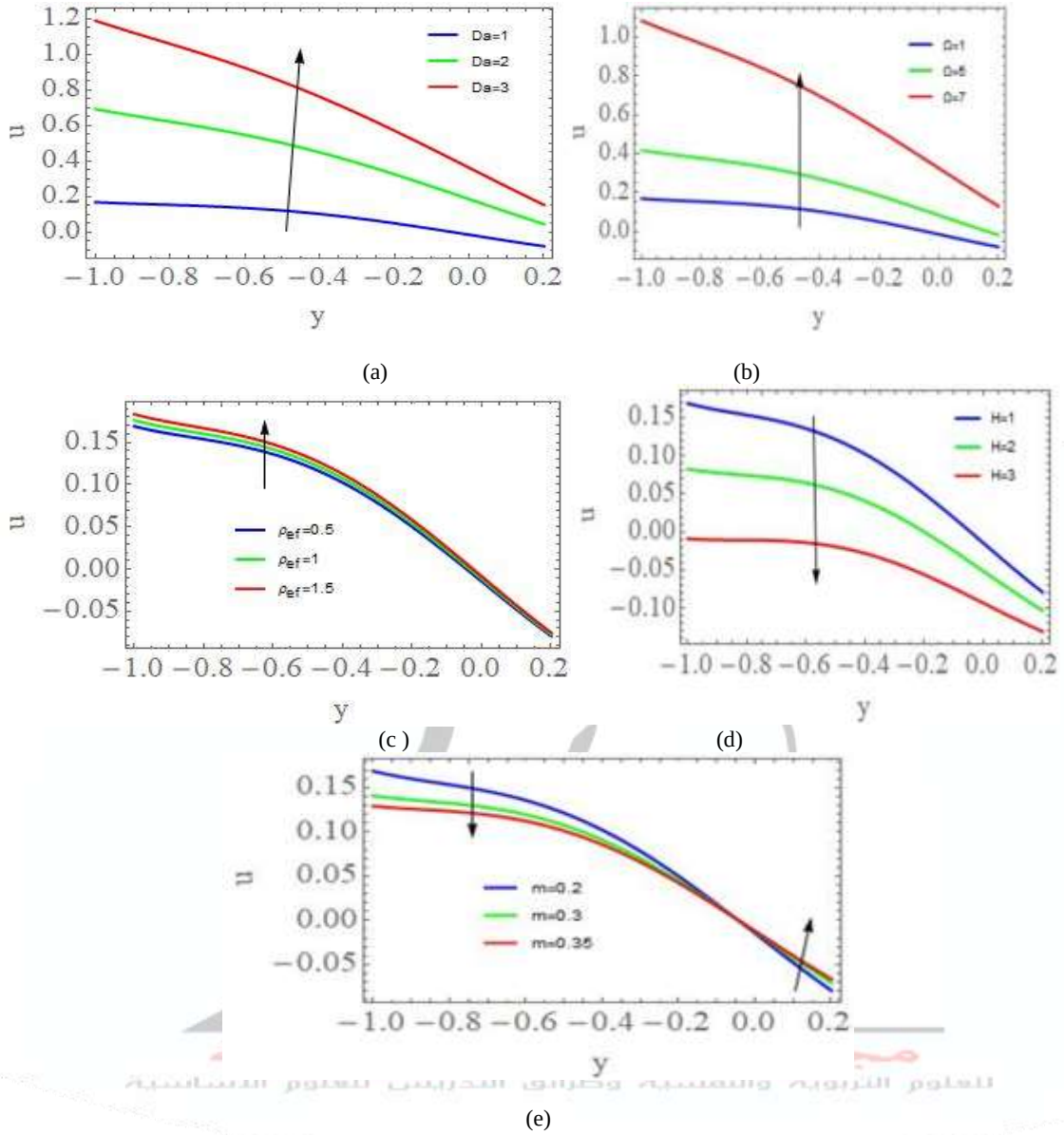


**Figure 6.** Variation the velocity profile with different perimeter "$u$"when $\{D_a \to 1, H \to 1, M \to 3, a_1 \to 0.6, a_2 \to 0.7, d \to 1, \phi \to \frac{\pi}{3}, F \to 1, W \to 0.2, m \to 0.2, \rho_{ef} \to 0.5, \Omega \to 1, \mu_f \to 0.5, d_1 \to 0.2, x \to 1\}$

### 3.3. Pressure Gradient Profile " $\frac{\partial \mathrm{p}}{\partial \mathrm{x}}$"

This subsection will examine the pressure within the canal. Each graphic in this section depicts the difference in pressure for variations along the channel at a specific wavelength x∈[-1,0]. The data indicates that the flow is constrained in the narrow section of the channel x∈[-0.5,-0.2]. A

JOBS
مجلة العلوم الأساسية
Journal of Basic Science
Print -ISSN 2306-5249
Online-ISSN 2791-3279
العدد الثامن والعشرون
٢٠٢٥م /١٤٤٦هـ

greater pressure gradient is necessary to attain normal flow. The reduced pressure gradient in the broader section of the canal x∈[-1, -0.5]∪[-0.2, 0] facilitates fluid passage. Figures 7 (a) and (b) show that the pressure gradient gets bigger as the Hartmann number $H$, and the non-uniform parameter $m$ go up. This graph indicates that greater pressure is necessary to transport a specific volume of fluid via the constricted section of the channel. Upon examining canal parameter, including the Darcy number $D_a$, rotation parameter $\Omega$, and effective density $\rho_{ef}$, as illustrated in Figure 7 (c-g), the observed pattern is reversed. The incline requires a reduced pressure of fluid movement.

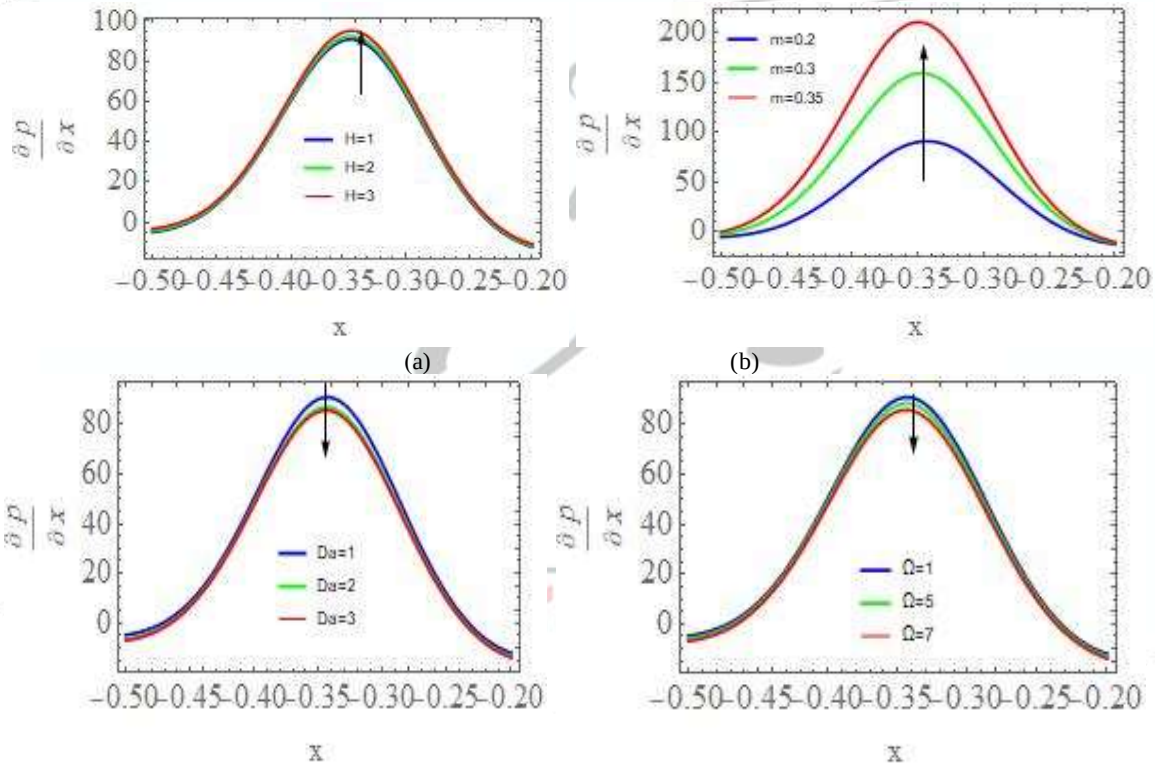


(a) (b)

(c) (d)

JOBS
مجلة العلوم الأساسية
Journal of Basic Science
Print -ISSN 2306-5249
Online-ISSN 2791-3279
العدد الثامن والعشرون
٢٠٢٥م /١٤٤٦هـ

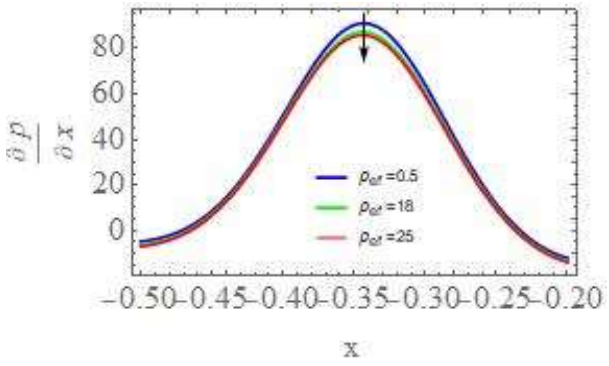


(e)

**Figure 7.** Variation the pressure gradient profile with different perimeter " $\frac{\partial p}{\partial x}$"when $\{D_a \to 1, H \to 1, M \to 3, a_1 \to 0.6, a_2 \to 0.7, d \to 1, \phi \to \frac{\pi}{3}, F \to 1, W \to 0.2, m \to 0.2, \rho_{\text{ef}} \to 0.5, \Omega \to 1, \mu_f \to 0.5, d_1 \to 0.2, y \to 1, F_r \to 0.5, \alpha \to \frac{\pi}{6}, R_e \to 0.1\}$

3.4. Temperature Profile "$\vartheta$ "

This subsection examines the effect of the different major physical parameters on the temperature profile in Figure 8 (a-c). The results indicate the nearly parabolic nature of the temperature profiles. Figure 8(a) shows the influence of heat absorption parameter $\beta$ on temperature profile. The findings show that there exists a considerable increase in the temperature of the fluid for the increasing value of heat absorption parameter $\beta$ in In the center of the channel and decreases on the sides. Afterward, heat transfer diffusion occurs due to random molecular motion, the adjacent molecules move less vigorously and thus transport less energy between them when they are extinguished. Notice in the figure 8( b) that when the thermal slip parameter $\gamma$ increases, the temperature decreases. As for the figure 8(c), the temperature decreases in the center of the channel with an increase on the sides of the channel when increasing effective thermal conductivity of hybrid nanomaterial $K$.

JOBS
مجلة العلوم الأساسية
Journal of Basic Science
Print -ISSN 2306-5249
Online-ISSN 2791-3279
العدد الثامن والعشرون
٢٠٢٥م/ ١٤٤٦هـ

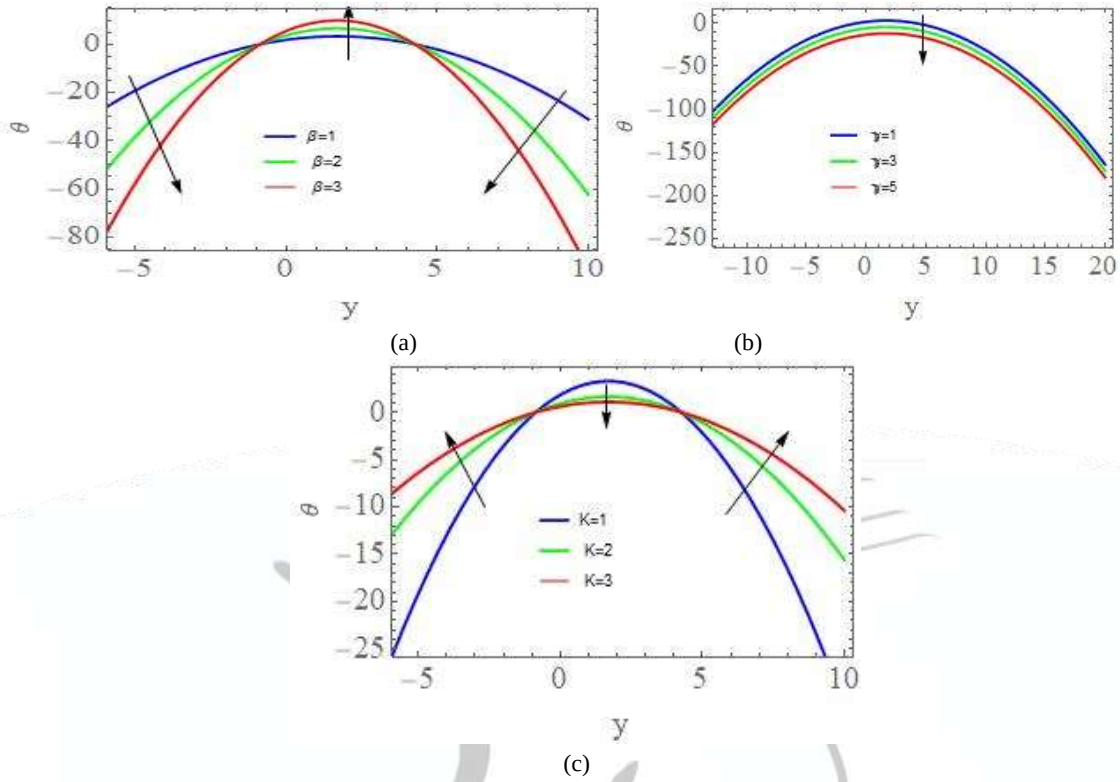


**Figure 8.** Variation the temperature profile with different perimeter "ϑ " when $\{a_1 \to 0.6, a_2 \to 0.7, m \to 0.7, d \to 1, \phi \to \frac{\pi}{6}, \gamma \to 1, \beta \to 1, K \to 1, x \to 1\}$

## 4. Conclusions

This paper investigated the peristaltic flow of hybrid nanomaterials in an inclined tapered channel, given the effects of rotation, porous media, and magnetohydrodynamics (MHD). The cumulative impact of heat transfer are being considered. We depicted the key variables in the study by graphing them with Mathematica (11.3) software and found the following results:

- Increased rotation of $\Omega$ and the Darcy number $D_a$ increases velocity and the volume of the entrapped mass, accompanied by a less pressure gradient.
- As the Hartmann number $H$ increases, the velocity and volume of the entrapped mass decrease and the pressure gradient escalates.
- As the non-uniform parameter $m$ increases, both the bolus volume and the pressure gradient increase, the velocity on the left side diminishes, and the velocity on the right side escalates.

- The pressure gradient reduces and the velocity increases as the effective density $\rho_{ef}$ increases.
- As the heat absorption parameter $\beta$ increases, the temperature escalates; conversely, an increase in both the effective thermal conductivity of the hybrid nanomaterial $K$ and the thermal slip parameter $\gamma$ helps decrease temperature.

## References

1. Abbasi, F. M., Gul, M., & Shehzad, S. A. (2020). Effectiveness of temperature-dependent properties of Au, Ag, Fe3O4, Cu nanoparticles in peristalsis of nanofluids. International Communications in Heat and Mass Transfer, 116, 104651.

2.Abd-Alla, A. M., & Abo-Dahab, S. M. (2015). Magnetic field and rotation effects on peristaltic transport of a Jeffrey fluid in an asymmetric channel. Journal of Magnetism and Magnetic Materials, 374, 680-689.

3.Abdulhussein, H., & Abdulhadi, A. M. (2023). Impact of Heat Transfer and Inclined MHD on A Non-Uniform Inclined Asymmetrical Channel with Couple Stress Fluid Through A Porous Medium. Iraqi Journal of Science, 4580-4599.

4.Alshareef, T. S. (2020, July). Impress of rotation and an inclined MHD on waveform motion of the non-Newtonian fluid through porous canal. In Journal of Physics: Conference Series (Vol. 1591, No. 1, p. 012061). IOP Publishing.

5. [Fung, Y. C., & Yih, C. S. (1968). Peristaltic transport .ASME J. Appl. Mech., 35 (4), 669–675.

6. Ibraheem, R. G., & Hummady, L. Z. (2024). Effect of Different Parameters on Powell-Eyring Fluid Peristaltic Flow with the Influence of a Rotation and Heat Transform in an Inclined Asymmetric Channel. Baghdad Science Journal, 21(4), 1318-1318.

7. Iftikhar, N., Rehman, A., Sadaf, H., & Iqbal, S. (2019). Study of Al2O3/copper–water nanoparticle shape, slip effects, and heat transfer on steady physiological delivery of MHD hybrid nanofluid. Canadian Journal of Physics, 97(12), 1239-1252.

8. Imran, N., Javed, M., Sohail, M., & Tlili, I. (2020). Utilization of modified Darcy's law in peristalsis with a compliant channel: applications to thermal science. Journal of Materials Research and Technology, 9(3), 5619-5629.

9.Latham, T. W. (1966). Fluid motions in a peristaltic pump (Doctoral dissertation, Massachusetts Institute of Technology.(

10. Nazeer, M., Irfan, M., Hussain, F., & Siddique, I. (2023). Entropy generation analysis in blood-gold casson nanofluid through horizontal wavy channel with velocity and thermal slips: applications in skin diseases. Journal of Computational Biophysics and Chemistry, 22(03), 259-272.

11. Noreen, S., Rashidi, M. M., & Qasim, M. (2017). Blood flow analysis with considering nanofluid effects in vertical channel. Applied Nanoscience, 7, 193-199.
12. Salih, A. W., & Abdulhadi, A. M. (2024). Influences of Irreversibility in Transport of Peristaltic of Hybrid Nanomaterial through a Porous Medium in an Inclined Channel. Iraqi Journal of Science, 5638-5652.
13. Salman, M. R. (2023, February). Effect of convective conditions in a radiative peristaltic flow of pseudoplastic nanofluid through a porous medium in a tapered an inclined asymmetric channel. In AIP Conference Proceedings (Vol. 2414, No. 1). AIP Publishing.
14. Shapiro, A. H., Jaffrin, M. Y., & Weinberg, S. L. (1969). Peristaltic pumping with long wavelengths at low Reynolds number. Journal of fluid mechanics, 37(4), 799-825.
15. Sheriff, S., Ahmad, S., & Mir, N. A. (2021). Irreversibility effects in peristaltic transport of hybrid nanomaterial in the presence of heat absorption. Scientific Reports, 11(1), 19697.
16. Sheriff, S., Mir, N. A., Ahmad, S., & Rafiq, N. (2021). Porosity and dissipative effects in Peristalsis of hydro-magneto nanomaterial: Application of biomedical treatment. Advances in Mechanical Engineering, 13(4), 16878140211011890.
17. Zahan, I., Nasrin, R., & Alim, M. A. (2019). Mixed convective hybrid nanofluid flow in lid-driven undulated cavity: effect of MHD and Joule heating. Journal of Naval Architecture and Marine Engineering, 16(2), 109-126.

JOBS
مجلة العلوم الأساسية
Journal of Basic Science
Print -ISSN 2306-5249
Online-ISSN 2791-3279
العدد الثامن والعشرون
٢٠٢٥م /١٤٤٦هـ